Magnetotransport in iodine-doped single-walled carbon nanotubes

Sejung Ahn and Yukyung Kim
Interdisciplinary Program in Nano-Science and Technology, Nano Systems Institute–National Core Research Center, Seoul National University, 599 Gwanak-ro, Gwanak-gu, Seoul 151-747, Korea

Youngwoo Nam, Honam Yoo, Jihyun Park, and Yungwoo Park
Department of Physics and Astronomy, Nano Systems Institute–National Core Research Center, Seoul National University, 599 Gwanak-ro, Gwanak-gu, Seoul 151-747, Korea

Zhiyong Wang and Zujin Shi
Beijing National Laboratory for Molecular Sciences, State Key Laboratory of Rare Earth Materials Chemistry and Applications, College of Chemistry and Molecular Engineering, Peking University, Beijing 100871, People's Republic of China

Zhaoxia Jin
Department of Chemistry, Renmin University of China, Beijing 100872, People's Republic of China
(Received 7 May 2009; revised manuscript received 28 July 2009; published 26 October 2009)

Magnetoresistance (MR) and magnetothermoelectric power (MTEP) of iodine-doped single-walled carbon nanotubes (I@SWNT) under magnetic fields up to 14 T are investigated from room temperature (300 K) down to 1.6 K. Our results on resistivity and thermoelectricpower (TEP) in a zero magnetic field are similar to those reported by Grigorian *et al.* [Phys. Rev. Lett. **80**, 5560 (1998)] The positive sign of the TEP values indicates that the majority of the carriers in the I@SWNT are holes. The broad enhancement of TEP at temperatures of 30–200 K shows quasilinear temperature dependence and is consistent with sharply varying density of states near the Fermi level with additional contribution from the spin-orbit scattering in the normal metallic characteristics of the I@SWNT. For $T<7$ K, MR is negative and it decreases with H^2 followed by the $H^{1/2}$ dependence at around $H=2$ T which is characteristic for the weak localization. In the range $7\ \mathrm{K}<T<70$ K, MR is positive at low magnetic field and becomes negative at higher magnetic field. The negative MR in the high magnetic fields decreases linearly. At $T\geq\sim 100$ K, MR is positive up to 14 T, which could be the result of spin-orbit scattering in the I@SWNT. The MTEP decreases under magnetic field at $T<90$ K. The reduction in MTEP is originated from the delocalization of electron wave functions under the magnetic field. At $T>90$ K, the thermal fluctuation dominates the effect of magnetic fields resulting the MTEP to be the same as the zero magnetic field TEP.

DOI: 10.1103/PhysRevB.80.165426 PACS number(s): 73.43.Qt, 72.20.Pa, 72.15.Rn

I. INTRODUCTION

Chemical modification of carbon nanotubes (CNTs) is important for application to the electronic devices because such chemical doping can shift the Fermi energy in the electronic band structure and can change the electronic properties of the host material.[1] Among the various chemical modification methods, manipulation through the combination of CNT and other molecules or polymers has been studied widely because a CNT has a large surface area and hollow structure. In particular, intercalation into the hollow space of CNT results in stable doping, in contrast to interstitial doping which is not stable. So far, many dopants such as iodine, boron, nitrogen, bromine, $FeCl_3$, Cs, K, C_{60}, poly(N-vinyl carbazole), polypyrrole, and polyacetylene have been doped into multiwalled nanotube (MWNT) and single-walled carbon nanotube (SWNT).[2–13]

Among the doped SWNT, iodine-doped SWNT (I@SWNT) are particularly interesting. The iodine is intercalated into the hollow space of SWNT, depending on the diameter of the SWNT, exists in the form of atomic chains or polymorphic structures inside the SWNT.[2,14] The I@SWNT forms an air stable charge-transfer compound. Iodine is a *p*-type dopant and when doped into SWNT forms an electron acceptor in the form of $(I_3)^-$ or $(I_5)^-$. Therefore, electron transfers from SWNT to iodine can generate free hole carriers. In previous studies of transport properties of I@SWNT,[3–5] Grigorian *et al.* reported a reduction by ~40-fold in direct current (dc) resistance and a reduction by ~fourfold in thermoelectric power at 300 K. However, the studies of Grigorian *et al.* were performed under zero magnetic field conditions. In this paper, we focus on temperature-dependent magnetoresistance (MR) and magnetothermoelectric power (MTEP) under magnetic fields up to 14 T.

MR is a powerful indicator of the intrinsic properties of CNT samples. To date, MR measurements of various types of CNT have been performed and in SWNT networks, negative MR with positive upturns have been observed. Those results have been explained by the variable range hopping and weak localization theories.[15] On the other hand, in MWNT mats, positive MR at high temperature and negative MR at low temperature have been reported, those results being explained by the two band model and the two-dimensional weak localization theory, repectively.[16] MTEP has been reported for SWNT mats. A reduction in TEP under magnetic fields up to 6.5 T has been reported at low temperatures.[17] However, there have been no magnetotransport studies for I@SWNT. In this paper, we present

temperature-dependent MR and MTEP values for I@SWNT mats under magnetic fields up to 14 T.

II. EXPERIMENT

The pristine SWNTs were produced by arc-discharge method. The anode was a graphite rod filled with a powder mixture of YNi_2 alloy and graphite with weight ratio of 1:10. The cathode was a pure graphite rod. The arc discharge was ignited between the graphite electrodes in 720 Torr He atmosphere. The SWNTs were generated in the discharge process and subsequently purified.[18] The I@SWNT samples were prepared by heating a mixture of SWNT bulk powder and iodine in an evacuated glass tube at 150 °C for 24 h. The excess iodine remaining on the SWNT surface was removed by washing with ethanol until the solvent became colorless. The structural characterization of the iodine-doped SWNT has been detailed in Ref. 2. In this paper, the intercalated iodine was confirmed by Raman measurement. Raman spectra were measured at room temperature in a back scattering geometry with a JY LabRam HR fitted with a liquid-nitrogen-cooled charge-coupled-device detector. The spectra were collected under ambient conditions using the 514.5 nm line of an Ar-ion laser.

Temperature-dependent resistivity was measured using platinum wire pressure contacts in a four-probe configuration. The samples were cut into 2 mm × 1 mm × 0.03 mm (I@SWNT) and 1 mm × 1 mm × 0.015 mm (pristine SWNT) rectangular bars. For measurement of resistivity, a programmable current source (Model 220A; Keithley Instruments, Cleveland, OH, USA) and a nanovoltmeter (Model 2182A; Keithley Instruments) were used. Temperature was controlled by a Neocera LTC-21 cryogenic temperature controller (Neocera, Front Royal, VA, USA). MR was measured by sweeping the magnetic fields up to 14 T at a rate of 0.466 T/min using an Oxford 14 T superconducting magnet (Oxford Instruments, Abingdon, UK). The magnetic field was applied perpendicular to the bias current. The TEP was measured using a dc method with pressure contact applied at fixed temperatures by a differential technique over a thermal gradient (typically $\Delta T = 1$ K).[19] As a heat source, a 220 Ω chip resistor was used to produce temperature differences in the dc method. We used a programmable current source (Model 220A; Keithley Instruments) and a digital voltmeter (Model 182; Keithley Instruments) for voltage measurement. Temperature variation was measured using a Lake Shore DRC-91CA temperature controller (Lake Shore Cryotronics, Westerville, OH, USA). The TEP data were corrected to account for the TEP provided by the copper leads. The MTEP was measured by applying an external magnetic field parallel to the temperature gradient using a Janis 7 T superconducting magnet (Janis Research Co. Wilmington, MA, USA).

III. RESULTS AND DISCUSSION

A. Raman scattering

Figure 1 shows the Raman spectra of pristine SWNT and I@SWNT taken by the 514.5 nm line of Ar-ion laser at 300 K. The spectra were normalized with *G*-band (tangential mode) peak intensities at 1597 cm^{-1} (I@SWNT) and 1594 cm^{-1} (pristine SWNT), respectively. Similar to the previous reports,[4,20] there are upshift of peaks to the high-frequency Raman modes, as a result of polyiodide chain intercalation in the SWNT. We did not observe any Raman peaks around 215 cm^{-1} which would be expected if iodine molecules were present in the samples.[21] It indicates that no excessive iodine exists in the sample. The new Raman peaks of I@SWNT were observed at 109 and 348 cm^{-1}, which were not detected in pristine SWNT. The Raman peak of I@SWNT near 172 cm^{-1} was stronger than that of pristine SWNT which could be contributed from $(I_5)^-$ polyiodide chain.[4] Also, since *D*-band (1358 cm^{-1}) peak corresponds to the defects mode and *G*-band (1597 cm^{-1}) peak corresponds to the graphite mode, the increase in the intensity ratio I_D/I_G of I@SWNT indicates that higher disorders are induced upon iodine doping.

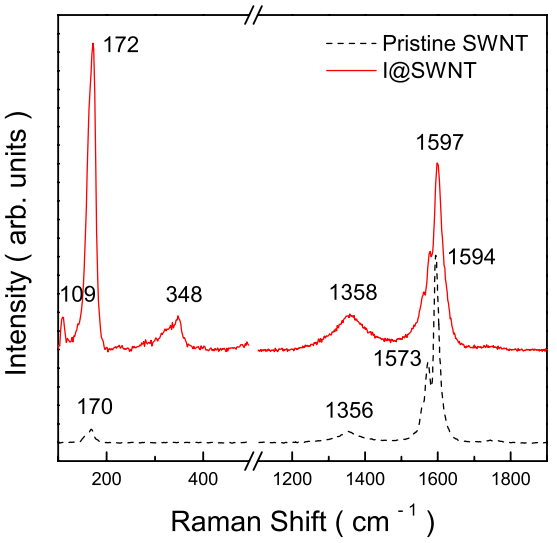

FIG. 1. (Color online) Raman spectra of pristine SWNT (black dashed line) and I@SWNT (red solid line) ($T = 300$ K, 514.5 nm excitation).

B. Resistivity at zero magnetic field

Figure 2(a) shows the temperature-dependent normalized resistivity of I@SWNT mats from room temperature (300 K) down to 1.6 K. The room temperature resistances were 0.5 and 3.2 Ω for I@SWNT and pristine SWNT, respectively [inset in Fig. 2(a)]. At high temperatures ($T > 180$ K), the temperature dependence of resistivity exhibits metallic behavior ($d\rho/dT > 0$) while below 180 K, nonmetallic behavior ($d\rho/dT < 0$) was observed [Fig. 2(a)]. This crossover pattern has been reported in doped CNT (Refs. 4 and 8) and doped polymers,[22,23] and can be explained by a heterogeneous model involving metallic resistivity and tunneling through small electrical barriers.[24,25] In a heterogeneous model, the general expression for resistivity can be written as

$$\rho(T) = \rho_m \exp\left(-\frac{T_m}{T}\right) + \rho_t \exp\left(\frac{T_t}{T + T_s}\right), \quad (1)$$

where the first term indicates a highly anisotropic metallic state and the second term corresponds to fluctuation-induced

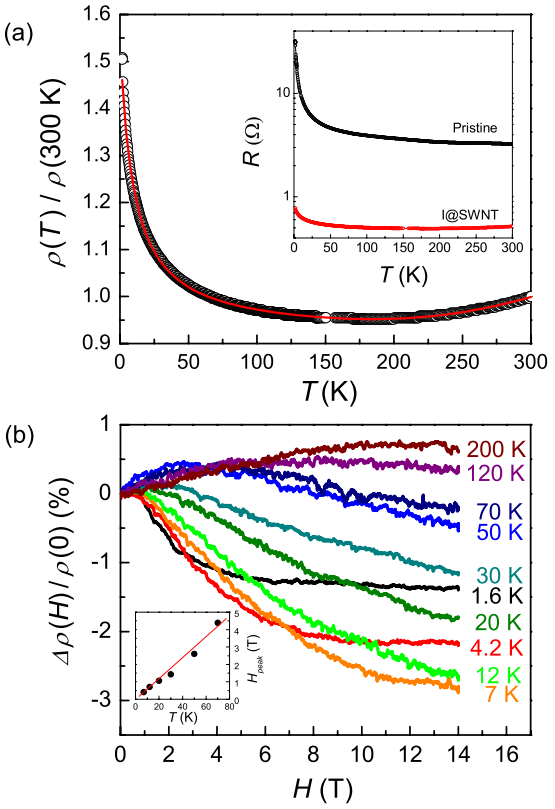

FIG. 2. (Color online) (a) Temperature dependence of resistivity of I@SWNT and curve fitted to a heterogeneous model. The parameters extracted from the fit and applied to Eq. (1) are ρ_m=0.013 Ω cm, ρ_t=0.0028 Ω cm, T_m=1253 K, T_t=6.87 K, and T_s=13 K; (inset) temperature dependence of resistance in pristine SWNT and I@SWNT. (b) MR of I@SWNT for 1.6 K$<T<$200 K; (inset) temperature dependence of positive MR peak position (red line added as a visual aid).

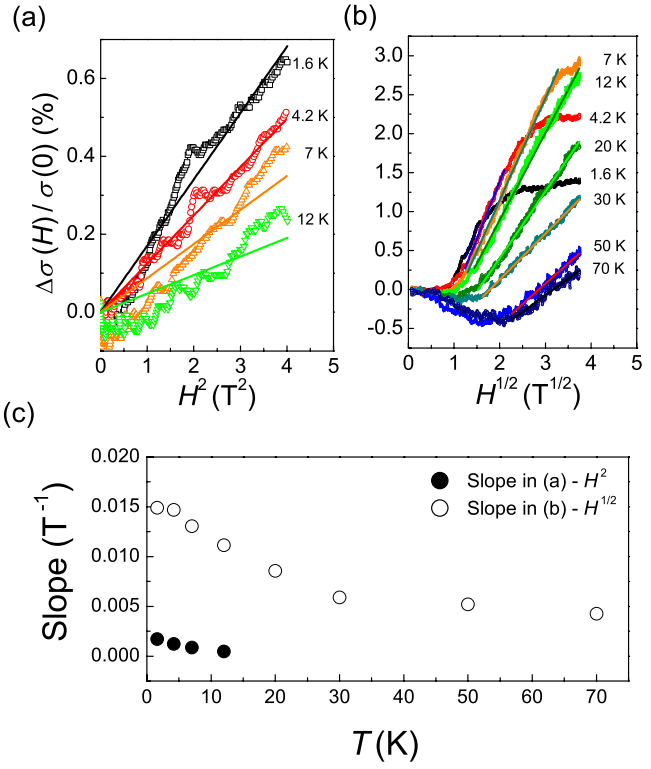

FIG. 3. (Color online) (a) $\Delta\sigma(H)/\sigma(0)$ versus H^2 plots in the low-field region ($H<2$ T) at 1.6, 4.2, 7, and 12 K. (b) $\Delta\sigma(H)/\sigma(0)$ versus $H^{1/2}$ plots in the high-field region at temperatures from 1.6 to 70 K. (c) Temperature dependence of the slope of the linear portions plotted in (a) (black dot) and (b) (empty dot).

tunneling between metallic regions separated by small barriers.[24–27] The parameter T_m gives the energy (k_BT_m) of phonons with wave vector $2k_F$ that can backscatter carriers. The parameter T_t is the temperature at which the amplitude of fluctuations is comparable to the barrier height. The parameter T_s is the temperature above which the thermally activated conduction over the potential barrier begins to occur. Therefore, the ratio T_t/T_s reflects the barrier size and the zero-temperature conductivity.[25,28] Resistivity versus temperature data are shown in Fig. 2(a): we note that the experimental curve is in good agreement with numerical fit by Eq. (1) with the following values of tunneling parameters, T_t=6.87 and T_s=13 K, which indicates that I@SWNT have large metallic regions separated by a thin tunneling barrier. The T_m value was 1253 K and the metallic term contribution at 180 K is only 0.4%, however, for $T>180$ K, the metallic contribution increases rapidly leading to $d\rho/dT>0$.

Thus, for $T>180$ K, metallic conduction along the I@SWNT is dominant. However, for $T<180$ K, intertube junctions or intratube defects can form small barriers and fluctuation-induced tunneling through the tubes becomes the dominant transport mechanism.

C. Magnetoresistance

Figure 2(b) shows the MR data in magnetic fields up to 14 T at different temperatures. For $T<7$ K, the MR was negative and decreased with H^2 following the $H^{1/2}$ dependence at around $H=2$ T which is characteristic for weak localization. In the range 7 K$<T<$70 K, the MR data were positive and exhibited a broad peak at low magnetic field and became negative at higher field. As temperature increases, the peak position of positive MR at low magnetic field is shifted to higher field and became broader [Fig. 2(b) inset]. Furthermore, the negative MR at high magnetic field decreases linearly. For $T\geq\sim100$ K, the MR was positive in magnetic fields up to 14 T. The MR increased linearly in a lower magnetic field and showed a broad peak in a high magnetic field [Fig. 2(b)].

The negative MR [i.e., positive magnetoconductance (MC)] at $T<70$ K is related to a weak localization effect. Weak localization predicts H^2-dependent MC for weak fields and $H^{1/2}$-dependent MC for strong field in a three-dimensional (3D) system.[29–33] In the case of I@SWNT, the MC has H^2 dependence for $H<2$ T below 12 K [Fig. 3(a)]. For small fields, $\Delta\sigma_{L,3D}(H,T)$ in a 3D system is given by[34]

$$\Delta\sigma_{L,3D}(H,T)=\frac{e^2}{96\pi^2\hbar}\left(\frac{4DeH}{\hbar c}\tau_0\right)^{3/2}\left(\frac{eH}{\hbar c}\right)^{1/2}\propto H^2, \quad (2)$$

where τ_0 is the phase coherence time and D is the diffusion coefficient that can be related to conductivity σ via the Ein-

stein relation, $\sigma = e^2 N(E_F) D$ in which $N(E_F)$ is the density of states at the Fermi level. On the other hand, in the high-field region, the MC data have $H^{1/2}$ dependence [Fig. 3(b)]. The $H^{1/2}$ dependence of the MC can be also related to localization effects. For large fields, $\Delta\sigma_{L,3D}(H,T)$ in a 3D system is given by[29]

$$\Delta\sigma_{L,3D}(H,T) \simeq 0.605 \frac{e^2}{2\pi^2\hbar}\left(\frac{eH}{\hbar c}\right)^{1/2} \propto H^{1/2}. \quad (3)$$

As temperature increases, $H^{1/2}$ dependence is weakened and becomes linear with H. Such linear H dependence could be the result of a nanojunction effect, which has been discussed for the linear MR observed in heavily doped polyacetylene.[33] In the mesh of I@SWNT, the nanojunction areas are formed by intertubular contact barriers.

The positive MR observed at high temperature is unusual and it can be the result of the spin-orbit scattering in the I@SWNT.[29,31,35] Iodine is generally known to have large spin-orbit coupling effect in various iodine intercalated compounds.[36,37] The spin-orbit scattering in I@SWNT could induce phase incoherence in the system leading to a positive MR. The positive peak at low magnetic field on top of the negative MR at 7 $\mathrm{K} < T < 70$ K could be from the positive MR contribution of the spin-orbit coupling added to the negative MR from the weak localization effect. The observed positive MR in the entire magnetic field regime at $T \geq \sim 100$ K confirms that the negative MR contribution originated from the weak localization is no longer important at this high temperature. As a result, the positive MR contribution of the spin-orbit coupling could be persisted to the high magnetic field regime at the high temperature.

D. Thermoelectric power and magnetothermoelectric power

Figure 4(a) shows the temperature dependence of TEP at zero magnetic field in pristine SWNT and I@SWNT for 2.5 $\mathrm{K} < T < 300$ K. The TEP is positive over the entire temperature range with +16 μV/K and +38 μV/K at room temperature for I@SWNT and pristine SWNT, respectively. The positive TEP indicates that the majority of the carriers in I@SWNT are holes. In previous reports[3,4] the TEP of CNT was observed to decrease following iodine doping, which suggested that iodine doping created free hole carriers. The broad enhancement of TEP at 30 $\mathrm{K} < T < 200$ K with quasilinear temperature dependence, as shown in Fig. 4(a), suggests sharply varying densities of states near the Fermi level in normal metallic diffusion thermoelectric power. The nonlinear temperature dependence of TEP may be explained by the effect of density-of-states peaks. The standard expression for TEP is given by[6,38,39]

$$S = \frac{1}{eT\sigma}\int \sigma(E)(E-\zeta)\frac{df}{dE}dE, \quad (4)$$

where σ is the conductivity, ζ is the chemical potential (assumed to be constant with temperature), e is the electronic charge, and f is the Fermi function. For the partial conductivity function, $\sigma(E)$, we use $\sigma(E) \sim N(E)\mu(E)$, as for a simple metallic system, where $N(E)$ is the density of states

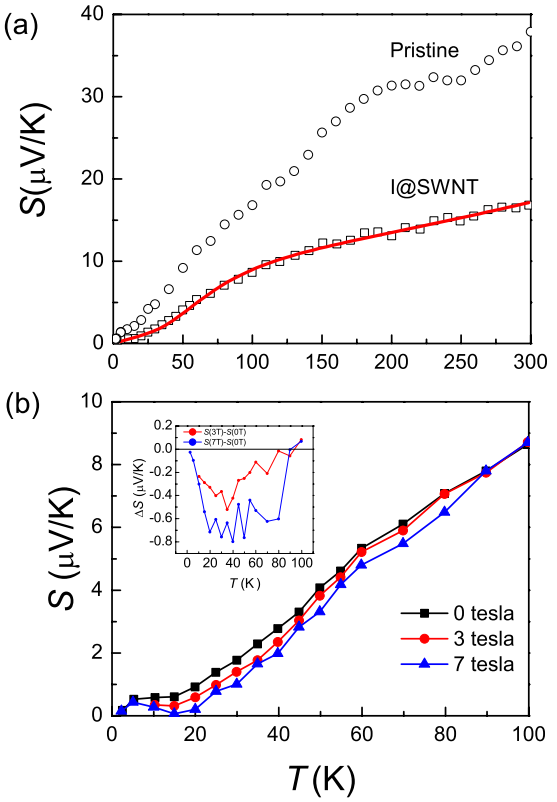

FIG. 4. (Color online) (a) Temperature dependence of TEP at zero magnetic field in pristine SWNT and I@SWNT. The red line shows the fit to the heterogeneous model. The parameters extracted from the fit and applied to Eq. (5) are $a=0.047$, $b=5.27\times10^6$, and $T_p=259.2$ K. (b) Temperature dependence of MTEP; (inset) $\Delta S(H)=S(H)-S(0)$ versus T.

and $\mu(E)$ is the energy-dependent carrier mobility. We assume that $\mu(E)$ is only weakly energy dependent within the width of the Fermi-energy window, as expected for elastic disorder scattering so that $\sigma(E) \sim N(E)$ and we can focus on the role that the density of states might play in affecting TEP.[40] There are sharply varying densities of states near the Fermi level and if the partial conductivity function is approximated to a delta function the TEP becomes nonlinear. The expression for nonlinear TEP may be given by[6,38]

$$S = aT + \frac{bT_p}{eT\sigma}\frac{\exp(T_p/T)}{[\exp(T_p/T)+1]^2}, \quad (5)$$

where aT is the linear metallic term, b is a constant, and $T_p=(E_p-\zeta)/k_B$ in which E_p is the energy at which the peak occurs and k_B is Boltzmann's constant. Equation (5) provides a good fit for the TEP data for I@SWNT with a narrow peak ($\sim$22 meV below the Fermi level) and is consistent with a previous analysis[38] of TEP data from I@SWNT reported by Grigorian *et al.*[4]

The MTEP was measured at $H=3$ and 7 T at $T<100$ K [Fig. 4(b)]. After the magnetic field was applied, the MTEP became smaller than the zero-field TEP. At $T<90$ K, the MTEP was approximately 0.6 μV/K smaller than the zero-field TEP value and it was the same as the zero-field TEP value at $T>100$ K. (The MTEP data at $T<5$ K were diffi-

cult to discriminate from the TEP data values since the absolute magnitude of both MTEP and TEP at this low temperature approaches zero.) Similar reductions in TEP have been reported in undoped SWNT at $T<250$ K.[17] If the magnetic scattering of charge carriers were important for the TEP at $T<90$ K, it can be reduced in the MTEP since spins are ordered under magnetic field resulting smaller entropy of the system. On the other hand, weakly localized electron wave functions can be delocalized under an applied magnetic field. Accordingly, in a disordered I@SWNT system under a magnetic field, the number of delocalized charge carriers increases resulting in smaller entropy, i.e., a reduction in TEP under magnetic field conditions. The delocalization model of localized electron wave functions under a magnetic field for the MTEP is consistent with the analysis of the MR results shown in Fig. 2(b). For $T>90$ K, the thermal fluctuation dominates the effect of magnetic fields and the MTEP value approaches the TEP value. The nonlinear term in TEP at the high temperature could be partially contributed by the spin-orbit scattering consistent with the observed positive MR in the delocalized metallic conduction regime at the high temperature.

IV. CONCLUSION

In summary, the resistivity of I@SWNT shows a crossover pattern from metallic to nonmetallic temperature dependence as temperature decreases. This pattern agrees with the heterogeneous model involving metallic resistivity and tunneling through small electrical contact barriers. The TEP measurement results show that I@SWNT has a metallic property and that the majority of the carriers are holes. The broad enhancement of TEP suggests the marked variation in the densities of states peaks near the Fermi level and the spin-orbit scattering effect due to iodine doping. The MR, measured in magnetic fields up to 14 T, was a function of temperature. The negative MR at $T<70$ K is consistent with the weak localization model while the positive MR observed at $T>7$ K is discussed as spin-orbit scattering effect in the I@SWNT. Furthermore, we observed a reduction in MTEP in the presence of a magnetic field, which suggests that an increase in delocalized charge carriers originates from delocalization of electron wave functions under the magnetic field. At $T>90$ K, the thermal fluctuation dominated the effect of magnetic fields resulting the MTEP to the same as the zero magnetic field TEP.

ACKNOWLEDGMENTS

This work was supported by the Korea Foundation for International Cooperation of Science and Technology (KICOS) through a grant provided by the Ministry of Education, Science and Technology (MEST), Korea (Grant No. GPPK20602000006-07E0200-00610) and by the Nano Systems Institute-National Core Research Center (NSI-NCRC) program of KOSEF.

[1] W. Liang, J. Yang, and J. Sun, Appl. Phys. Lett. **86**, 223113 (2005).
[2] L. Guan, K. Suenaga, Z. Shi, Z. Gu, and S. Iijima, Nano Lett. **7**, 1532 (2007).
[3] L. Grigorian, G. U. Sumanasekera, A. L. Loper, S. Fang, J. L. Allen, and P. C. Eklund, Phys. Rev. B **58**, R4195 (1998).
[4] L. Grigorian, K. A. Williams, S. Fang, G. U. Sumanasekera, A. L. Loper, E. C. Dickey, S. J. Pennycook, and P. C. Eklund, Phys. Rev. Lett. **80**, 5560 (1998).
[5] L. Grigorian, G. U. Sumanasekera, A. L. Loper, S. L. Fang, J. L. Allen, and P. C. Eklund, Phys. Rev. B **60**, R11309 (1999).
[6] Y.-M. Choi, D.-S. Lee, R. Czerw, P.-W. Chiu, N. Grobert, M. Terrones, M. Reyes-Reyes, H. Terrones, J.-C. Charlier, P. M. Ajayan, S. Roth, D. L. Carroll, and Y.-W. Park, Nano Lett. **3**, 839 (2003).
[7] D. L. Carroll, Ph. Redlich, X. Blasé, J.-C. Charlier, S. Curran, P. M. Ajayan, S. Roth, and M. Rühle, Phys. Rev. Lett. **81**, 2332 (1998).
[8] R. S. Lee, H. J. Kim, J. E. Fischer, A. Thess, and R. E. Smalley, Nature (London) **388**, 255 (1997).
[9] V. Z. Mordkovich, M. Baxendale, S. Yoshimura, and R. P. H. Chang, Carbon **34**, 1301 (1996).
[10] B. W. Smith, M. Monthioux, and D. E. Luzzi, Nature (London) **396**, 323 (1998).
[11] J. Steinmetz, S. Kwon, H. J. Lee, E. Abou-Hamad, R. Almairac, C. Goze-Bac, H. Kim, and Y. W. Park, Chem. Phys. Lett. **431**, 139 (2006).
[12] J. Steinmetz, H. J. Lee, S. Kwon, D. S. Lee, C. Goze-bac, E. Abou-Hamad, H. Kim, and Y. W. Park, Curr. Appl. Phys. **7**, 39 (2007).
[13] L. Duclaux, Carbon **40**, 1751 (2002).
[14] X. Fan, E. C. Dickey, P. C. Eklund, K. A. Williams, L. Grigorian, R. Buczko, S. T. Pantelides, and S. J. Pennycook, Phys. Rev. Lett. **84**, 4621 (2000).
[15] G. T. Kim, E. S. Choi, D. C. Kim, D. S. Suh, Y. W. Park, K. Liu, G. Duesberg, and S. Roth, Phys. Rev. B **58**, 16064 (1998).
[16] S. N. Song, X. K. Wang, R. P. H. Chang, and J. B. Ketterson, Phys. Rev. Lett. **72**, 697 (1994).
[17] E. S. Choi, D. S. Suh, G. T. Kim, and Y. W. Park, Synth. Met. **103**, 2504 (1999).
[18] H. J. Li, L. Feng, L. H. Guan, Z. J. Shi, and Z. N. Gu, Solid State Commun. **132**, 219 (2004).
[19] Y. W. Park, Synth. Met. **45**, 173 (1991).
[20] A. M. Rao, P. C. Eklund, Shunji Bandow, A. Thess, and R. E. Smalley, Nature (London) **388**, 257 (1997).
[21] R. C. Teitelbaum, S. L. Ruby, and T. J. Marks, J. Am. Chem. Soc. **101**, 7568 (1979).
[22] Y. W. Park, E. S. Choi, and D. S. Suh, Synth. Met. **96**, 81 (1998).
[23] Kwanghee Lee, Shinuk Cho, Sung Heum Park, A. J. Heeger, Chan-Woo Lee, and Suck-Hyun Lee, Nature (London) **441**, 65 (2006).
[24] A. B. Kaiser, G. Dusberg, and S. Roth, Phys. Rev. B **57**, 1418 (1998).

[25] A. B. Kaiser, G. C. McIntosh, K. Edgar, J. L. Spencer, H. Y. Yu, and Y. W. Park, Curr. Appl. Phys. **1**, 50 (2001).
[26] P. Sheng, Phys. Rev. B **21**, 2180 (1980).
[27] A. B. Kaiser, Adv. Mater. **13**, 927 (2001).
[28] G. McIntosh, Ph.D. thesis, Victoria University of Wellington, 2000.
[29] Patrick A. Lee and T. V. Ramakrishnan, Rev. Mod. Phys. **57**, 287 (1985).
[30] L. Piraux, V. Bayot, X. Gonze, J.-P. Michenaud, and J.-P. Issi, Phys. Rev. B **36**, 9045 (1987).
[31] Reghu M., K. Väkiparta, Y. Cao, and D. Moses, Phys. Rev. B **49**, 16162 (1994).
[32] D.-S. Suh, T. J. Kim, A. N. Aleshin, Y. W. Park, G. Piao, K. Akagi, H. Shrakawa, J. S. Qualls, S. Y. Han, and J. S. Brooks, J. Chem. Phys. **114**, 7222 (2001).
[33] V. I. Kozub, A. N. Aleshin, D.-S. Suh, and Y. W. Park, Phys. Rev. B **65**, 224204 (2002).
[34] A. N. Aleshin, V. I. Kozub, D.-S. Suh, and Y. W. Park, Phys. Rev. B **64**, 224208 (2001).
[35] B. Kramer and A. MacKinnon, Rep. Prog. Phys. **56**, 1469 (1993).
[36] M. Lee, H. Kim, Y. S. Lee, and M. S. Kim, Angew. Chem., Int. Ed. **44**, 2929 (2005).
[37] M. Atanasov, C. Rauzy, P. Baettig, and C. Daul, Int. J. Quantum Chem. **102**, 119 (2005).
[38] A. B. Kaiser, Y. W. Park, G. T. Kim, E. S. Choi, G. Düsberg, and S. Roth, Synth. Met. **103**, 2547 (1999).
[39] J. S. Dugdale, *The Electrical Properties of Metals and Alloys* (Edward Arnold, Paris, 1997).
[40] J. Y. Lee, G. C. McIntosh, A. B. Kaiser, Y. W. Park, M. Kaack, J. Pelzl, Chul Koo Kim, and Kyun Nahm, J. Appl. Phys. **89**, 6223 (2001).